Arabian Journal of Chemistry (2022) **15**, 103631

King Saud University

Arabian Journal of Chemistry

www.ksu.edu.sa
www.sciencedirect.com

ORIGINAL ARTICLE

Development of superior antibodies against the S-protein of SARS-Cov-2 using macrocyclic epitopes

Hassan Traboulsi [a,*], **Mohammed A. Khedr** [b,c], **Rafea Elgorashe** [a], **Yasair Al-Faiyz** [a], **Amr Negm** [a,d]

[a] *Department of Chemistry, College of Science, King Faisal University, P.O Box 400, Al-Ahsa 31982, Saudi Arabia*
[b] *Department of Pharmaceutical Sciences, College of Clinical Pharmacy, King Faisal University, Al-AHasa 31982, Saudi Arabia*
[c] *Department of Pharmaceutical Chemistry, Faculty of Pharmacy, Helwan University, P.O. Box 11795, Cairo, Egypt*
[d] *Biochemistry Division, Chemistry Department, Faculty of Science, Mansoura University, Mansoura, Egypt*

Received 27 March 2021; accepted 6 December 2021
Available online 10 December 2021

KEYWORDS

SARS-CoV-2;
Spike protein;
Receptor binding domain;
Epitopes;
Macrocyclic peptides;
Molecular dynamics;
Antibodies;
Inhibition

Abstract One of the proven methods to prevent and inhibit viral infections is to use antibodies to block the initial Receptor Binding Domain (RBD) of SARS-CoV-2 S protein and avoid its binding with the host cells. Thus, developing these RBD-targeting antibodies would be a promising approach for treating the SARS-CoV-2 infectious disease and stop virus replication. Macrocyclic epitopes constitute closer mimics of the receptor's actual topology and, as such, are expected to be superior epitopes for antibody generation. This work demonstrated the vital effect of the three-dimensional shape of epitopes on the developed antibodies' activity against RBD protein of SARS-CoV-2. The molecular dynamics studies showed the greater stability of the cyclic epitopes in comparison with the linear counterpart, which was reflected in the activity of their produced antibodies. Indeed, the antibodies we developed using macrocyclic epitopes showed superiority with respect to binding to RBD proteins compared to antibodies formed from a linear peptide. The results of the present work constitute a roadmap for developing superior antibodies that could be used to inhibit the activity of the SARS-CoV-2 and prevent its reproduction.

1. Introduction

The coronavirus disease 2019 (COVID-19) is caused by severe acute respiratory syndrome coronavirus 2 (SARS-CoV-2 virus), that first started in Wuhan, China in December 2019. (Rodriguez-Morales et al., 2020) Nowadays the virus has reached a pandemic level and represents a threat to global health. There is no specific antiviral agents for the treatment

* Corresponding author at: Department of Chemistry, College of Science, King Faisal University, Al-Ahsa 31982, Saudi Arabia.
E-mail address: htraboulsi@kfu.edu.sa (H. Traboulsi).
Peer review under responsibility of King Saud University.

Production and hosting by Elsevier

https://doi.org/10.1016/j.arabjc.2021.103631
1878-5352

of COVID-19. The treatment is symptomatic, and oxygen therapy represents the first step for addressing respiratory impairment. Other therapies, e.g., Corticosteroids for the treatment of viral pneumonia or acute respiratory distress syndrome (ARDS) have been also used in this context Several anti-flu drugs, some antiviral and immunomodulatory therapy were associated with viral load reduction until viral disappearance. Besides, some inflammation inhibitors have shown promising roles in improving oxygenation in a majority of patients (Cavalli et al., 2020, Roschewski et al., 2020). Meanwhile, scientific research is growing to develop several types of vaccines against Sars-CoV-2 (Zhu et al., 2020). Although the development of vaccines showed a rapid progress, many questions about their effectiveness and productions are raised and need more investigations (Krammer, 2020; Zeng et al., 2020). Passive immunization is applied today using polyclonal antibodies from convalescent donors, for fighting COVID-19, mainly in patients with immune-deficient conditions (Levi-Schaffer & de, 2021). Additionally, it has been shown that multiple human antibodies were efficient in neutralizing SARS-Cov-2 and inhibited its infectious activity in cultured systems. Different proteins are encoding Corona viruses, including S (spike), M (membrane), E (envelope), and N (nucleocapsid) (Wang et al., 2020b) Indeed, The viral entry into host cells is mediated through the binding between the cell angiotensin-converting enzyme 2 (ACE2) receptor and the Receptor Binding Domain (RBD) of the virus in the S1 subunit followed by a fusion between the virus and the cell through the S2 subunit of the protein (Ni et al., 2020). Thus, the S protein is highly considered as a promising target for discovering efficient antibodies, entry inhibitors, and vaccines (Huang et al., 2020, Dai & Gao, 2021). The production of antibodies against S protein is achieved by immunization the animal models with recombinant S-protein of SARS-CoV-2.(Lu et al., 2020) Other researchers have considered, more specifically, the receptor-binding domain (RBD) to develop neutralizing antibodies against SARS-Cov-2 (Liu et al., 2020). Despite the encouraging results in the above-mentioned approaches, it would be more important to consider specific epitopes in the production of highly selective and superior antibodies against the S protein of SARS-CoV-2. Indeed, using big pathogens such as attenuated microorganisms or recombinant proteins may result in harmful immune responses and undesired side effects (Purcell et al., 2007). Considering this reductionist approach, the most specific neutralizing antibodies are expected to be obtained in an epitope-peptide based strategy. These epitopes should constitute the minimal immunogenic region of the protein and allow the production of more specific neutralizing antibodies. The first step in our approach of antibody production is the epitope selection, which determines specificity, selectivity, and sensitivity. In this regard, we considered the reported crystal structure of RBD bound to the cell receptor ACE2 where our focus was on the RBD sequences that are interaction with ACE2 (Lan et al., 2020). Linear peptides currently used to elicit antibodies' production have numerous confirmations that do not reflect the topology of the native protein. On the other hand, macrocycles are large rings possessing restricted conformations similar to original structures found in proteins (Hill et al., 2014). Molecular dynamic is an effective computational tool widely used to evaluate the conformational stability of newly discovered therapeutics. It was recently employed to prove the secondary structure and establish the excellent stability of the tested SARS-CoV2 peptide inhibitor. Additionally, molecular dynamics were used in the *in silico* investigation of a number of peptide inhibitors of SARS-CoV-2 spike protein (Panda et al., 2021).

In this work, we have prepared linear and macrocyclic peptidomimetics as conformational epitope mimics (MEM: Macrocyclic Epitope Mimics) for the production of superior antibodies against S protein of SARS-CoV-2 for therapeutic and diagnostic applications. The effect of the epitope structure and its stability on the antibody activity was examined by molecular dynamics studies. Although the project initially targets the RBD of S protein of SARS-CoV-2 to develop neutralizing antibodies for therapeutic and diagnostic use, this project's methodology could be directly transferable to discover other antibodies that can target other regions and proteins encoding the surface of SARS-Cov-2.

2. Methods

2.1. Design of peptides

Conformational searches were performed using the Low-Mode MD application from the "Molecular Operating Environment" software MOE 2016.08 (Computing & Inc, 2016). The reported crystal structure of the SARS-Cov-2 RBD in complex with ACE2 has allowed us to select the sequences with good interactions and can be used as epitopes for neutralizing antibody development (Lan et al., 2020). The topology of these regions was an important parameter for peptide selection. It is worth noting that the used SARS-Cov-2 RBD was the one discovered at the time we started the project, and this is the reason why it was selected in this work. The details are the following: Gene: (S) UNQ 868/PRO1885; Mutations = 0; Uniport code = P0DTC2; PDB ID = 2M0J. The stability of the selected peptides after initial energy minimization and after MD simulation was important parameter as well. In addition, the presence of cysteine residues was another parameter that allowed the formation of macrocyclic peptides through disulfide formation.

2.2. Molecular dynamics

All molecular dynamic (MD) simulations were conducted by MOE software (Computing & Inc, 2016). The dynamics simulations were applied for a conformational search to find out the stable conformation and calculate the RMSD for each designed peptide. The quality of the temperature-related factors, protein geometries, and electron density were tested. All hydrogens were added, and energy minimization was computed. The solvent molecules in the system were deleted before solvation, and salt atoms were added to ensure complete neutralization of the biomolecular system. The solvent atoms were added to surround the system in a cubic shape. Amber 10:EHT was selected as a force field in the potential setup step. All Van der Waals forces, electrostatics, and restraints were enabled. The heat was adjusted to increase the temperature of the system from 0 to 300 K, followed by equilibration. Cooling was then initiated until 0 K was reached. The simulation was conducted over 50 ns period of time. The 3D structure of peptides was built, and the protonation state was checked. Partial charges were calculated. Energy was minimized using a suit-

able forcefield. The topology problems were solved. The system was surrounded by a cube shape of solvent (water), and NaCl was used as a salt to neutralize charged system. Amber12: EHT was selected as an all-atom forcefield. All bonds, Van Der Waals, electrostatics, and restraints were enabled. Energy minimization was performed. Root mean square deviation gradient was 1.0. Start time was zero, and the checkpoint was 250. The molecular dynamics protocol was done using NPA (Nose-Poincare-Andersen) to solve the equation of motion. Temperature was 300 K, and the time scale was 50000 ps (50 ns).

2.3. Peptide synthesis

One Linear and two macrocyclic counterpart peptides have been synthesized. The synthesis was performed on Rink Amide MBHA Resin using the Fmoc solid-phase peptide approach and orthogonal protecting groups were carefully chosen. The sequences of peptides are presented in Table 1.

Cyclization of peptides was performed through disulfide formation between the side chains of the cysteine amino acids. For example, for the synthesis of the semi cyclic peptide **(2)**, the sequence CNGVEGFNCY-NH_2 was first assembled on resin using orthogonal protecting groups. The oxidization was made then between the two Cysteine on the resin by using Iodine in DMF, and the synthesis was continued after that to complete the desired sequence. The same strategy was applied for the synthesis of the second cyclic peptide **(3)**. The three peptides were cleaved from the Rink amid resin and the protecting groups were removed simultaneously using the mixture TFA/TIS/water (95:2.5:2.5). The three peptides bear a terminal cysteine to conjugate them to the immunogenic BSA protein.

2.4. HPLC analysis

In order to verify the purity of the synthesized peptides, HPLC Analyses were carried out. All the experiments were conducted on CXTH LC3050N system coupled with a UV–Visible detector. Successful purifications of samples were achieved by gradient elution on a reverse-phase Gemini-NX 5µ C- 18 110A, 4.6*250 mm column, using a mobile phase consisting of 0.1 %Trifluoroacetic in 100% Acetonitrile and 0.1 %Trifluoroacetic in 100% Water at a detection wavelength of 220 nm, Flow rate: 1.0 ml/min and volume: 20 µl. CXTH data system software was used to control the HPLC system and for data acquisition and analysis. The gradient mobile phase set for the different peptides is presented in (SI, Table S1). All the peptides were obtained with a purity greater than 90% as shown in the HPLC spectra (SI, Figures S1, S2 and S3).

Table 1 Sequences of the studied peptides. All the peptides bear a cysteine for bioconjugation with the immunogenic protein BSA. **[]** represents the place of cyclization in the macrocycles. **Z** represents the spacer amino hexanoic acid.

Peptide's #	Peptide's sequence	Peptide's shape
(1)	C-Z-YQAGSTPSNGVEGFNSY-NH_2	Linear
(2)	C-Z-YQAGSTP[CNGVEGFNC]Y-NH_2	Semi cyclic
(3)	C-Z-[CYQAGSTPSNGVEGFNSYC]–NH_2	Cyclic

2.5. LC-MS spectrometry

Peptides' masses were verified by LC-MS (SI, Figures S4, S5, and S6). The analyses were carried out using Agilent 6125B (ESI) LC/MS. The detection was conducted by an MS equipped with a V electrospray ionization (ESI) source, and the following MS parameters are applied: Nebulizer Gas Flow: 1.5 L/min CDL: −20.0 v CDL Temp: 250 Co Block Temp.: 200 Co Probe Bias: +4.5kv Detector: 1.5 kv and Flow rate: 0.2 ml/min. The separation of samples was achieved by isocratic elution on a reverse-phase Gemini-NX 5µ C- 18 110A, 4.6*250 mm column, using a mobile phase consisting of 50 % H_2O / 50 % acetonitrile. Agilent Open LAB CDS software was used to control the MS data acquisition and analysis.

2.6. Immunization and antibody production

Immunization and boosts (in duplicate) of New Zealand White rabbits for 70 days have been done at Proteogenix (Schiltigheim, France, https://www.proteogenix.science) to produce polyclonal antibodies against the different synthesized epitopes. The experiments on animals were conducting according to the regulations of ISO9001:2015 Quality Management System and the ARRIVE Guidelines (https://arriveguidelines.org). Proteogenix respects the ethical use of animal science and their applied protocols are accredited by the Association for Assessment and Accreditation of Laboratory Animal Care International (AAALAC). Each antibody was produced in duplicate in two different rabbits. For this purpose, six rabbits (randomly female and male) with average body weight 2 kg ± 200 g were used. The rabbits were housed in metal cages separately, where fresh and clean water was supplied. The peptides have been conjugated to a BSA immunogenic protein through the terminal cysteine and injected in the rabbits. The sera have been collected, and biweekly ELISA measurements against the corresponding epitopes were performed to detect the antibody production.

2.7. Direct ELISA on the collected sera

0.5 µg of the RBD was typically immobilized to a 96-well microliter plate via a chemical reaction that results in the covalent attachment of the antigen through free amino groups. Detection is then performed in three steps, which include probing the coated well with equal volumes of sera. This step is followed by probing the bound antibody using a secondary antibody (1:8000) specific for the constant region of the primary antibody. The secondary antibody is typically conjugated to alkaline phosphatase, which can be readily detected using a colorimetric substrate reaction. The color change is then analyzed in a plate reader in a UV–visible spectrophotometer equipped to detect changes in absorbance after different sera dilution. Value of 0.200 in absorbance was considered a threshold of detection.

2.8. Antigen-specific antibody purification

The produced antibodies in the pooled rabbits' sera were purified using affinity chromatography technique in which antibody-containing sera were filleted to remove any large interfering particles. The sera were then passed through protein G-coupled Sepharose columns then the resulted eluted solutions were passed through agarose beads immobilized with peptides which are specific for the required antibody. Then, the unbounded nonspecific antibodies were washed out with a low salt solution. After that, the targeted antibody is eluted from the beads and assessed for binding to the specific antigen using ELISA. The concentrations of the produced antibodies were determined by UV–visible spectrophotometry and Beer-Lambert equation.

2.9. Sodium dodecyl sulfate polyacrylamide gel electrophoresis (SDS-PAGE)

The collected fractions were analyzed by SDS-PAGE under reducing and non-reducing conditions at neutral pH. The concentration of polyacrylamide gel was 12%. Samples were incubated with 2% SDS for 10 mins at 100 °C. Afterward, 200 ng from each sample were loaded onto the polyacrylamide gel wells. The electrophoresis analyses were done using electrophoresis instrument (Bio-Rad Laboratories, USA). After complete separation, the gel was stained with Coomassie Brilliant Blue G 250, and a further distaining step was performed.

2.10. Western blot analysis of antibodies against RBD

The recombinant RBD was purchased from Proteogenix (RBD purity and sequence are presented in SI, Figure S7). RBD was electrophoresed on an 8% SDS-PAGE gel and transferred to a nitrocellulose membrane by blotting. The membrane was blocked by bovine Serum Albumin (BSA) protein. The RBD protein was detected by adding the purified antibodies and washed, then incubated with secondary antibodies and visualized by adding horseradish peroxidase HRP –specific substrate, and the color was developed.

3. Results

3.1. Peptide design and synthesis

The linear and macrocyclic peptidic sequences have been selected and designed based on the RBD-ACE2 X-Ray structure.(Lan et al., 2020)

The structures of the peptides matching the native sequence in the RBD protein were visualized using MOE software (Computing & Inc, 2016) and are presented in Fig. 1. The synthesis of the designed peptides was successfully achieved with a purity greater than 90%, as calculated from HPLC analyses (SI, Figures S1, S2, and S3). The physicochemical properties of these peptides are presented in SI section (Table S2). The peptides showed isoelectric points less than 7.4 (optimum blood pH), which may correct or antagonize the poor solubility effect.

3.2. Molecular dynamics

All the designed peptides were subjected to MD simulations over 50 ns period of time. The trajectories were analyzed, and the root mean square deviation (RMSD Å) values were computed. According to the results, the semi-cyclic peptide **(2)** showed the least RMSD = 0.61 Å compared with 1.52 Å and 2.00 Å for peptides **(3)** and **(1),** respectively. Peptide **(2)** achieved stability after 20 ns (Fig. 2I), and this stability was continuous till the end of MD. Its equilibrium was obtained at least deviation0.61 Å. For peptide **(2)**, it was important to analyze the relaxed and non-relaxed conformations of the cysteine-cysteine bridge before and after equilibrium. The angles were also measured to examine the configuration of the stable conformations (Fig. 2II). The angle of Cys-Cys bridge in **(2)** was 104.2° and then became 95.0° at equilibrium in its most stable form (Fig. 2II).

3.3. Polyclonal antibody productions

After immunization of the three synthesized peptides in rabbits for 70 days, all the sera were collected. The ELISA studies against the corresponding epitope were performed to verify the presence of antibodies (SI, Figure S10). The ELISA results confirmed the presence of antibodies in the different collected sera. The extraction of the obtained antibodies has been achieved by purification through antigen conjugated resin which is known to increase the detection sensitivity and reduce the undesirable background. All the antibodies have been purified, and their concentrations have been calculated to be in the range of 1 $mg.ml^{-1}$. The purified antibodies were obtained in duplicate and denoted **A01**, **A02,** and **A03** in correspondence with peptides **(1)**, **(2),** and **(3)**. The antibodies were preserved in PBS buffer, 0.02% sodium azide, pH 7.4. Additionally, their activities against their corresponding epitopes have been verified by ELISA technique. The purity of the different antibodies has been checked by SDS-PAGE in reducing and non-reducing conditions, as shown in Fig. 3.

3.4. Western Blot and ELISA analyses against RBD

To figure out the recognition between the different produced antibodies and the RBD, Western Blot analyses have been performed, as shown in Fig. 4.

To compare the different antibodies' affinity toward the RBD, ELISA studies have been performed on the three antibodies. The obtained results are shown in Fig. 5.

The EC50 or the concentration of antibodies that give half maximal binding were calculated from ELISA curves for **A01**, **A02,** and **A03**. The obtained values were 4.10, 0.39, and 1.30 for antibodies **A01**, **A02,** and **A03,** respectively.

4. Discussion

The present work aimed to prepare linear and macrocyclic peptidomimetics as conformational epitope mimics (MEM: Macrocyclic Epitope Mimics) to produce superior polyclonal antibodies against S protein of COVID-19 for therapeutic

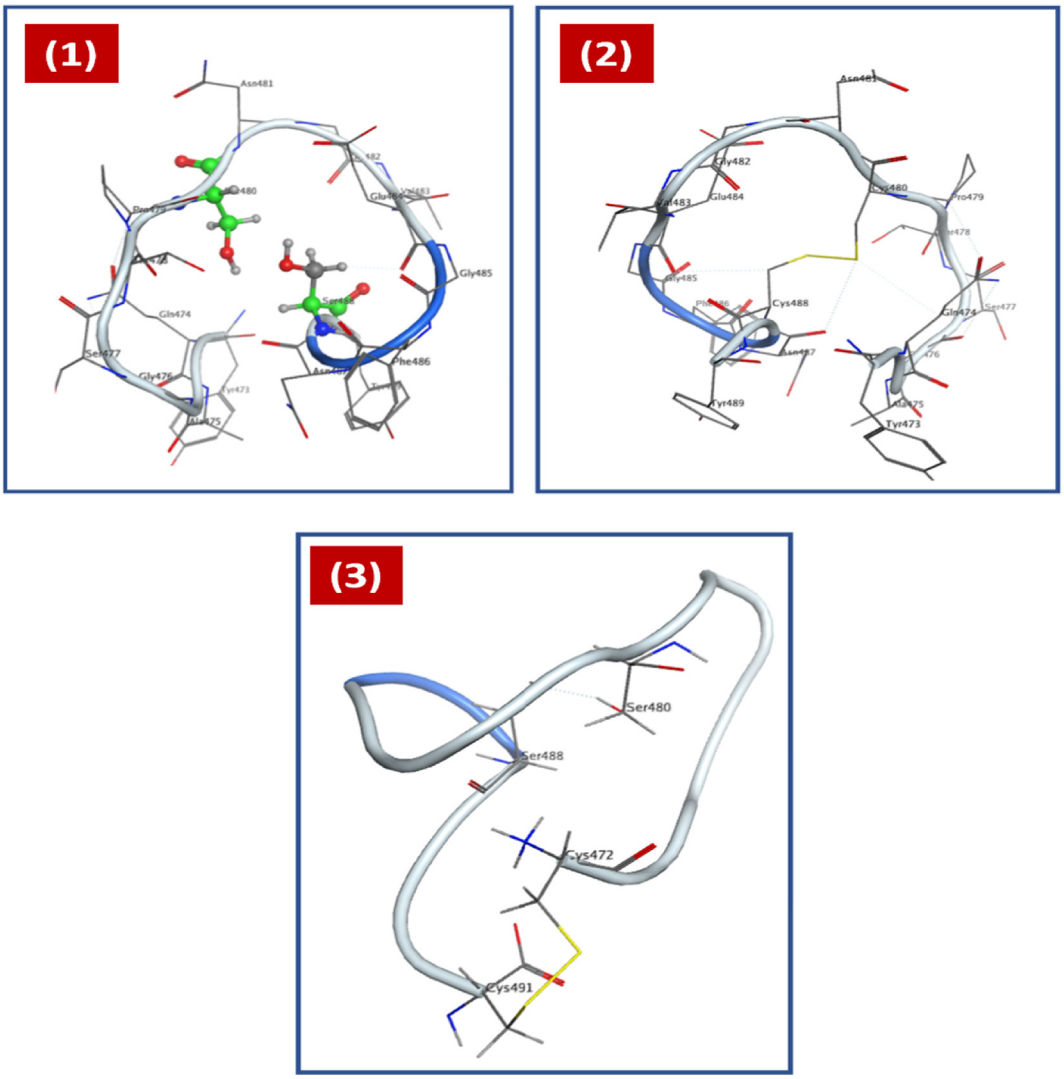

Fig. 1 Structures of the designed peptides **(1)**, **(2)** and **(3)** matching with the native sequences in RBD.

and diagnostic applications. Fundamentally, the approach relies on the fact that a cyclic, conformationally restricted peptide is a more faithful mimic of the actual 3D topology of surface protein domains than a linear peptide and thus a superior epitope for antibody generation (Gueret et al., 2020). The reported crystallographic structure of the complex between SARS-Cov-2 RBD and ACE2 has allowed us to select the sequences that could be used as epitopes for neutralizing antibody development (Lan et al., 2020; Shang et al., 2020). Our sequences are selected from the Receptor Binding Motif (RBM) and, more specifically, on one of the regions (Tyr473-Tyr489), which contains four residues interacting with ACE2 (Lan et al., 2020; Shang et al., 2020). The RBD of SARS-Cov-2 has a twisted five-stranded antiparallel β sheet with short connecting helices and loops that together form the core. A total of nine cysteine amino acids are found in RBD structure, eight of which form four pairs of disulfide bridges that appear in the final model. The remaining pair located in our targeted region (Cys480–Cys488) connects the loops in the distal end of the RBM (Lan et al., 2020). The RBD is a promising target for virus inhibition. It was chosen as a prototype in this project for several reasons: First, the RBD plays an important role in Cell penetration. Secondly, the Crystal structure of the RBD of SARS-COV in complex with the human receptor ACE2 is reported. Thirdly, the RBD of SARS-Cov-2 has been recently characterized and the amino acid sequences homology was found to be 77.5% with the protein of the SARS-COV (Wang et al., 2020c). One Linear and two cyclic counterparts were selected to be examined in the framework of this project. The three peptides were engineered to have a terminal Cysteine for conjugation with the immunogenic BSA protein. In order to avoid the two internal cysteine and their interactions with BSA, they were replaced with two serine (the amino acid the most similar to cysteine). According to the MD results, peptide **(2)** was predicted to be the top ranked in stability greater than the cyclic peptide **(3)** and the linear peptide **(1)** that showed higher deviation values (Fig. 2, SI, Figures S8, and S9). The equilibrium in case of the linear peptide **(1)** was achieved after a longer time than in **(2)** and **(3)**. The main reason for that may refer to that the linear peptide features more flexible conformations, and as a result, it also showed the highest RMSD value of 2.00 Å

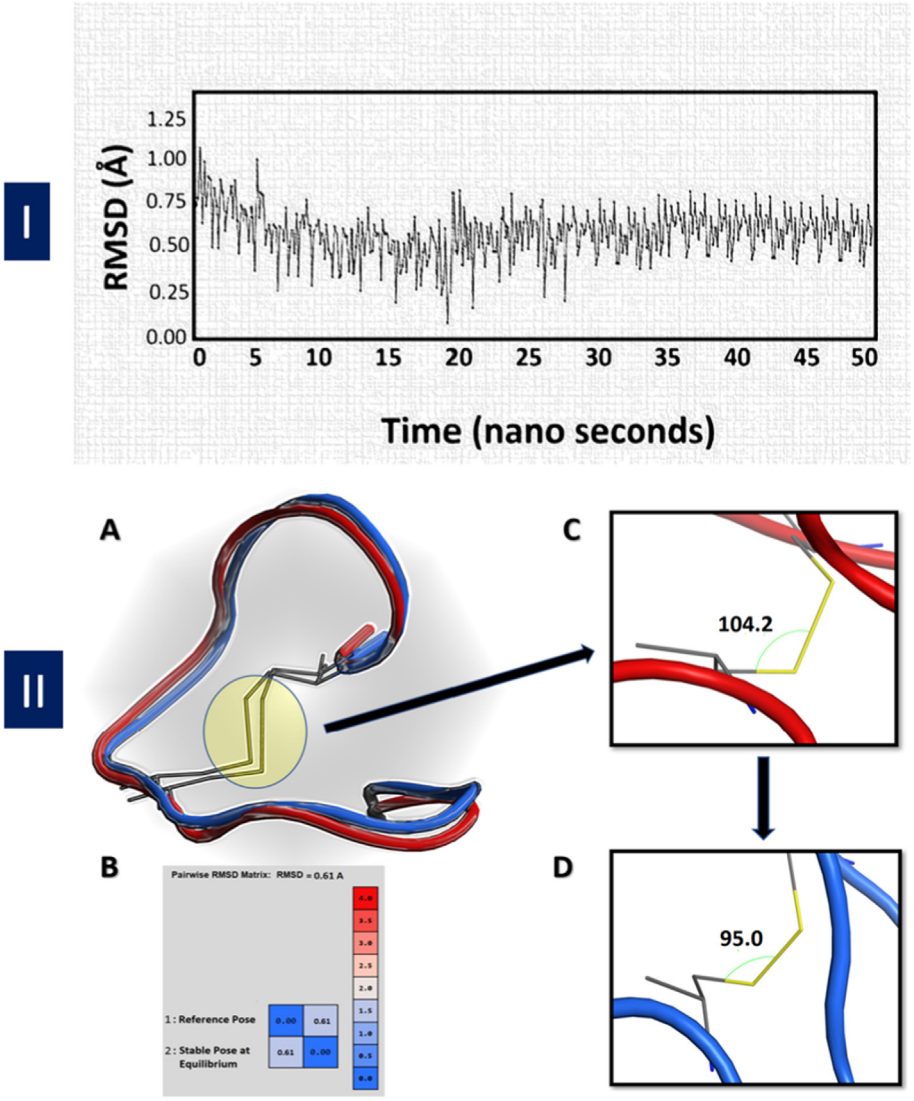

Fig. 2 I) MD of peptide **(2)** over 50 ns showing the least RMSD = 0.61 Å. II) A) Superimposition of the reference conformation of peptide **(2)** (red) and the stable one at equilibrium (blue), B) RMSD matrix, C) Measured angle before MD, D) Measured angle after MD. Peptide **(1)** showed the least stability as it reached equilibrium after a long time of 35 ns (SI, Figure S8). Peptide **(3)** achieved stability after 30 ns with RMSD 1.52 Å (SI, Figure S9). The angle of Cysteine-Cysteine bridge in **(3)** was 118.7°, and then it became 102.8°at equilibrium in its most stable form (SI, Figure S9).

(Fig. 2). Comparing **(2)** and **(3)**, the MD calculations showed greater stability for peptide **(2),** indicating the important effect of the sulfur-sulfur bridge between the two internal cysteine on the epitope stability (SI, Figures S8, and S9). The ELISA data on the sera have shown that all the immunized epitopes have generated antibodies with different responses (SI, Figure S10). At a constant volume of analysis, the data showed some significant differences in the results of the antibodies against their corresponding epitopes. This could be related either to the difference in antibody generation, concentration, or the antibody - epitope affinity. The extraction of the antibodies has been achieved by purification with corresponding antigen conjugated resin. The SDS-PAGE in reducing and non-reducing conditions for the obtained antibodies has allowed us to estimate the purity of the different antibodies to be more than 95% (Fig. 3). The affinities of our antibodies toward the recombinant RBD protein have been confirmed with Western Blot analyses, where all the studied samples have shown a clear antibody-RBD binding (Fig. 4). The ELISA studies conducted on the different antibodies against the RBD confirmed the binding observed in Western Blot. Additionally, the EC50 values calculated from the ELISA data showed significant differences depending on the used epitope for antibody generation (Fig. 5). Although the three peptides we used to generate these antibodies have similar sequences, one can see an important effect of the peptide 3D conformational structure on the activity of the produced antibodies. Indeed, the linear peptide, most probably due to its high flexibility, has led to the production of a less binding antibody (**A01**) against the RBD compared with its semi cyclic (**A02**) or cyclic (**A03**) counterparts. This can be seen from the EC50 values presented in Table 2, where the antibody generated from the semi cyclic peptide appears to

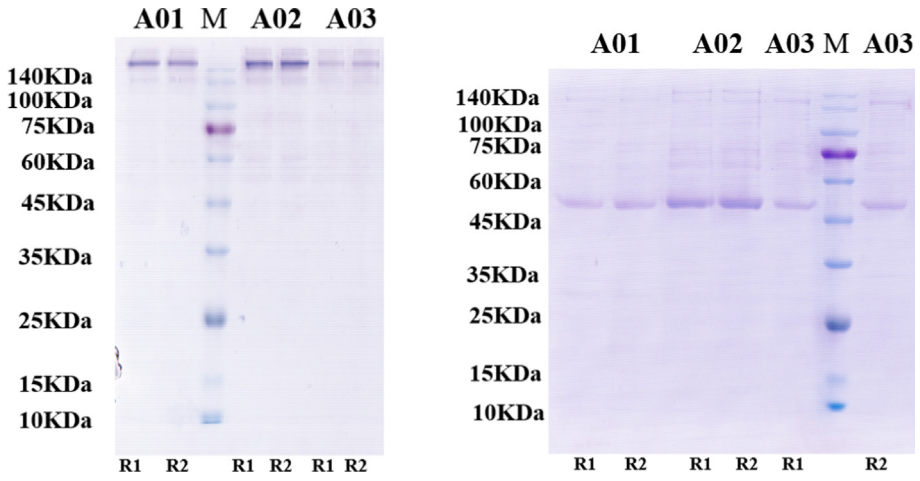

Fig. 3 SDS-PAGE for the produced antibodies**A01**, **A02,** and **A03** in I) non-reducing and II) reducing conditions. Each antibody has been prepared in duplicate R1 (Rabbit 1) and R2 (Rabbit 2). M is a pre-stained molecular weight marker.

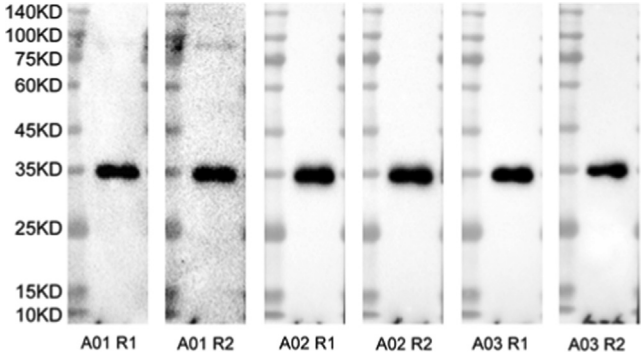

Fig. 4 Western Blot Analyses of antibodies **A01**, **A02,** and **A03**against the RBD protein. Each antibody has been produced in duplicate (Rabbit 1 (R1) and Rabbit 2 (R2)).

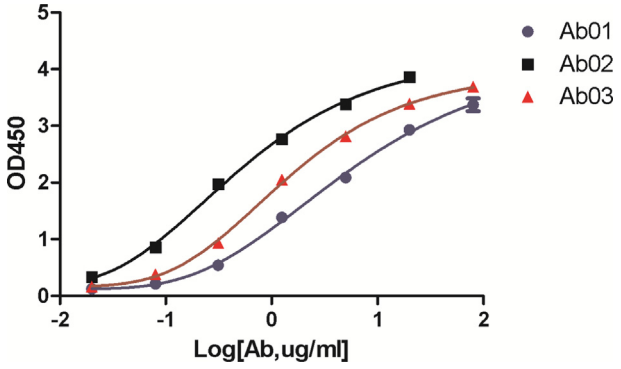

Fig. 5 ELISA of the purified antibodies **A01**, **A02 and A03** against the RBD.

have ten times more affinity toward RBD than the antibody of the linear peptide. These results are in perfect agreement with the MD calculations where **(2)** showed the least RMSD = 0.61 Å among the three peptides and has led to the obtention of the antibody with a greater affinity toward RBD (Table 2).

Table 2 EC50 of the three antibodies against the RBD protein and Epitope's RMSD (from MD).

Antibody	EC50	Epitope's RMSD (Å)
A01	4.10	2.00
A02	0.39	0.61
A03	1.30	1.52

The Sulfur- Sulfur bridge between Cys480–Cys488 appears to be fundamental for peptide structure stabilization and for a better mimic of the native confirmation found in the RBD. To the best of odxcddur knowledge, there is no previous reported work that showed the effect of the 3D conformational structure of the used epitope in the antibody production against SARS-Cov-2. Our technology will provide much-needed improved antibodies. It will also produce currently missing tools able to elucidate the target more accurately. This technology will allow the identification of new avenues for drug discovery against COVID-19.

5. Conclusion

In this work, we have designed linear and macrocyclic epitopes used for polyclonal antibody production against the S protein of SARS-Cov-2. The design was focused on one of the regions of RBD that show interactions with ACE2. MD simulations exhibited an important effect of the cyclization on the dynamic stabilities, allowing us to predict the antibodies with the greatest activities. The synthesized peptides were used to stimulate the production of antibodies in rabbits. Polyclonal antibodies were generated, purified, and characterized by Western Blot and ELISA techniques against the RBD. In agreement with the MD calculations, the antibodies developed using macrocyclic epitopes showed superior binding affinity toward RBD proteins compared to antibodies formed from the linear peptide. Our results should pave the way towards the development of superior antibodies that could be used to inhibit the activity of SARS-Cov-2.

Acknowledgments

The researchers would like to thank King Abdulaziz City for Science and Technology in Saudi Arabia (KACST) for the generous financial support through the COVID-19 fast research track (research grant # 5-20-01-004-0005)

Appendix A. Supplementary material

Supplementary data to this article can be found online at https://doi.org/10.1016/j.arabjc.2021.103631.

References

Cavalli, G., Ripa, M., Rovere-Querini, P., Ciceri, F., Landoni, G., Zangrillo, A., Dagna, L., Cavalli, G., De, L.G., Campochiaro, C., Della-Torre, E., Boffini, N., Tomelleri, A., Farina, N., Dagna, L., Ripa, M., Canetti, D., Oltolini, C., Castiglioni, B., Tassan, D.C., Scarpellini, P., Ruggeri, A., Ciceri, F., Rovere-Querini, P., Di, L. G., Martinenghi, S., Scotti, R., Tresoldi, M., Landoni, G., Zangrillo, A., 2020. Lancet Rheumatol 2, e325–e331.

Computing, C. & Inc, G. (2016). *Molecular operating environment (MOE)*.

Dai, L., Gao, G.F., 2021. Nat. Rev. Immunol. 21, 73–82.

Gueret, S.M., Thavam, S., Carbajo, R.J., Potowski, M., Larsson, N., Dahl, G., Dellsen, A., Grossmann, T.N., Plowright, A.T., Valeur, E., Lemurell, M., Waldmann, H., 2020. J. Am. Chem. Soc. 142, 4904–4915.

Hill, T.A., Shepherd, N.E., Diness, F., Fairlie, D.P., 2014. Angew. Chem Int. Ed. 53, 13020–13041.

Huang, Y., Yang, C., Xu, X.-F., Xu, W., Liu, S.-W., 2020. Acta Pharmacol. Ahead of Print, Sin.

Krammer, F., 2020. Nature (London, U. K.) 586, 516–527.

Lan, J., Ge, J., Yu, J., Shan, S., Zhou, H., Fan, S., Zhang, Q., Shi, X., Wang, Q., Zhang, L. & Wang, X. (2020). Nature (London, U. K.) 581, 215-220.

Levi-Schaffer, F. & de, M. A. (2021). Br. J. Pharmacol.

Liu, Z., Xu, W., Xia, S., Gu, C., Wang, X., Wang, Q., Zhou, J., Wu, Y., Cai, X., Qu, D., Ying, T., Xie, Y., Lu, L., Yuan, Z., Jiang, S., 2020. Signal Transduction Targeted Ther. 5, 282.

Lu, Y., Wang, Y., Zhang, Z., Huang, J., Yao, M., Huang, G., Ge, Y., Zhang, P., Huang, H., Wang, Y., Li, H., Wang, W.J., 2020. Immunol. Res. 9465398.

Ni, W., Bao, J., Li, R., Yang, D., Xu, Y., Cao, Z., Gao, Z., Yang, X., Yang, D., Xiao, Y., Hou, C., Wang, H., Liu, J., 2020. Crit Care 24, 422.

Panda, S.K., Sen Gupta, P.S., Biswal, S., Ray, A.K., Rana, M.K., 2021. J. Proteome Res. 20, 1296–1303.

Purcell, A.W., McCluskey, J., Rossjohn, J., 2007. Nat. Rev. Drug Discovery 6, 404–414.

Rodriguez-Morales, A.J., Bonilla-Aldana, D.K., Balbin-Ramon, G.J., Rabaan, A.A., Sah, R., Paniz-Mondolfi, A., Pagliano, P., Esposito, S., 2020. Infez. Med. 28, 3–5.

Roschewski, M., Lionakis, M. S., Sharman, J. P., Roswarski, J., Goy, A., Monticelli, M. A., Roshon, M., Wrzesinski, S. H., Desai, J. V., Zarakas, M. A., Collen, J., Rose, K., Hamdy, A., Izumi, R., Wright, G. W., Chung, K. K., Baselga, J., Staudt, L. M. & Wilson, W. H. (2020). Sci. Immunol. 5, eabd0110.

Shang, J., Ye, G., Shi, K., Wan, Y., Luo, C., Aihara, H., Geng, Q., Auerbach, A. & Li, F. (2020). Nature (London, U. K.) 581, 221-224.

Wang, N., Jiang, S., Du, L., Shang, J., Jiang, S., 2020b. Front Microbiol 11, 298.

Wang, Q., Zhang, Y., Wu, L., Niu, S., Song, C., Zhang, Z., Lu, G., Qiao, C., Hu, Y., Yuen, K.Y., Wang, Q., Zhou, H., Yan, J., Qi, J., 2020c. Cell 181, (894–904) e899.

Zeng, H., Wang, D., Nie, J., Liang, H., Gu, J., Zhao, A., Xu, L., Lang, C., Cui, X., Guo, X., Zhou, C., Li, H., Guo, B., Zhang, J., Wang, Q., Fang, L., Liu, W., Huang, Y., Mao, W., Chen, Y., Zou, Q., 2020. Signal Transduction Targeted Ther. 5, 219.

Zhu, F.C., Li, Y.H., Guan, X.H., Hou, L.H., Wang, W.J., Li, J.X., Wu, S.P., Wang, B.S., Wang, Z., Wang, L., Jia, S.Y., Jiang, H.D., Wang, L., Jiang, T., Hu, Y., Gou, J.B., Xu, S.B., Xu, J.J., Wang, X. W., Wang, W., Chen, W., 2020. Lancet 395, 1845–1854.

Further reading

Baig, M.S., Alagumuthu, M., Rajpoot, S., Saqib, U., 2020. Drugs R D 20, 161–169.

Bimonte, S., Crispo, A., Amore, A., Celentano, E., Cuomo, A., Cascella, M., 2020. In Vivo 34, 1597–1602.

Buonaguro, F.M., Puzanov, I., Ascierto, P.A., 2020. J. Transl. Med. 18, 165.

Cao, B., Wang, Y., Wen, D., Liu, W., Wang, J., Fan, G., Ruan, L., Song, B., Cai, Y., Wei, M., Li, X., Xia, J., Chen, N., Xiang, J., Yu, T., Bai, T., Xie, X., Zhang, L., Li, C., Yuan, Y., Chen, H., Li, H., Huang, H., Tu, S., Gong, F., Liu, Y., Wei, Y., Dong, C., Zhou, F., Gu, X., Xu, J., Liu, Z., Zhang, Y., Li, H., Shang, L., Wang, K., Li, K., Zhou, X., Dong, X., Qu, Z., Lu, S., Hu, X., Ruan, S., Luo, S., Wu, J., Peng, L., Cheng, F., Pan, L., Zou, J., Jia, C., Wang, J., Liu, X., Wang, S., Wu, X., Ge, Q., He, J., Zhan, H., Qiu, F., Guo, L., Huang, C., Jaki, T., Hayden, F. G., Horby, P. W., Zhang, D. & Wang, C. (2020). JAMA, J. Am. Med. Assoc. 323, 1787-1799.

Chen, N., Zhou, M., Dong, X., Qu, J., Gong, F., Han, Y., Qiu, Y., Wang, J., Liu, Y., Wei, Y., Xia, J.-A., Yu, T., Zhang, X., Zhang, L., 2020a. Lancet 395, 507–513.

Chen, X., Li, R., Pan, Z., Qian, C., Yang, Y., You, R., Zhao, J., Liu, P., Gao, L., Li, Z., Huang, Q., Xu, L., Tang, J., Tian, Q., Yao, W., Hu, L., Yan, X., Zhou, X., Wu, Y., Deng, K., Zhang, Z., Qian, Z., Chen, Y., Ye, L., 2020b. Cell. Mol. Immunol. 17, 647–649.

Dong, Y., Dai, T., Wei, Y., Zhang, L., Zheng, M., Zhou, F., 2020. Signal Transduction Targeted Ther. 5, 237.

Duan, K., Liu, B., Li, C., Zhang, H., Yu, T., Qu, J., Zhou, M., Chen, L., Meng, S., Hu, Y., Peng, C., Yuan, M., Huang, J., Wang, Z., Yu, J., Gao, X., Wang, D., Yu, X., Li, L., Zhang, J., Wu, X., Li, B., Xu, Y., Chen, W., Peng, Y., Hu, Y., Lin, L., Liu, X., Huang, S., Zhou, Z., Zhang, L., Wang, Y., Zhang, Z., Deng, K., Xia, Z., Gong, Q., Zhang, W., Zheng, X., Liu, Y., Yang, H., Zhou, D., Yu, D., Hou, J., Shi, Z., Chen, S., Chen, Z., Zhang, X., Yang, X., 2020. Proc. Natl. Acad. Sci. U. S. A. 117, 9490–9496.

Gautret, P., Lagier, J.-C., Honore, S., Hoang, V.T., Colson, P., Raoult, D., 2021. Int. J. Antimicrob. Agents 57, 106243.

Gordon, C.J., Tchesnokov, E.P., Feng, J.Y., Porter, D.P., Gotte, M., 2020. J. Biol. Chem. 295, 4773–4779.

HASSAN, A. M. B. P.-L. G. S. L. J.-F. L. F. M. E. N.-T. M.-É. S. P. T., 2020.

Kabra, R., Singh, S., 2021. Biochim. Biophys. Acta, Mol. Basis Dis. 1867, 165978.

Ledford, H., 2020. Nature (London, U. K.) 582, 469.

Mehraeen, E., Salehi, M. A., SeyedAlinaghi, S., Behnezhad, F. & Moghaddam, H. R. (2020). Infect Disord Drug Targets.

Salazar, E., Perez, K.K., Ashraf, M., Chen, J., Castillo, B., Christensen, P.A., Eubank, T., Bernard, D.W., Eagar, T.N., Long, S.W., Subedi, S., Olsen, R.J., Leveque, C., Schwartz, M.R., Dey, M., Chavez-East, C., Rogers, J., Shehabeldin, A., Joseph, D., Williams, G., Thomas, K., Masud, F., Talley, C., Dlouhy, K.G., Lopez, B.V., Hampton, C., Lavinder, J., Gollihar, J.D., Maranhao, A.C., Ippolito, G.C., Saavedra, M.O., Cantu, C.C., Yerramilli, P., Pruitt, L., Musser, J.M., 2020. Am. J. Pathol. 190, 1680–1690.

Shah, S.G.S., Farrow, A., 2020. Int. J. Surg. 76, 128–129.
Sharma, O., Sultan, A.A., Ding, H., Triggle, C.R., 2020. Front. Immunol. 11, 585354.
Shen, C., Wang, Z., Zhao, F., Yang, Y., Li, J., Yuan, J., Wang, F., Li, D., Yang, M., Xing, L., Wei, J., Xiao, H., Yang, Y., Qu, J., Qing, L., Chen, L., Xu, Z., Peng, L., Li, Y., Zheng, H., Chen, F., Huang, K., Jiang, Y., Liu, D., Zhang, Z., Liu, Y., Liu, L.J.A.M.A., 2020. J. Am. Med. Assoc. 323, 1582–1589.
Wang, C., Li, W., Drabek, D., Okba, N.M.A., van Haperen, R., Osterhaus, A.D.M.E., van Kuppeveld, F.J.M., Haagmans, B.L., Grosveld, F., Bosch, B.-J., 2020a. Nat. Commun. 11, 2511.
Wu, Y., Wang, F., Shen, C., Peng, W., Li, D., Zhao, C., Li, Z., Li, S., Bi, Y., Yang, Y., Gong, Y., Xiao, H., Fan, Z., Tan, S., Wu, G., Tan, W., Lu, X., Fan, C., Wang, Q., Liu, Y., Zhang, C., Qi, J., Gao, G.F., Gao, F., Liu, L., 2020. Science 368, 1274–1278.